JAST, Vol. 14, No. 2, pp.

JAST Journal of Aerospace Science and Technology

Science Article

Design and Vehicle Test of a Modified Predictive Kalman Filter for SINS Self Accurate Initial Alignment

Nemat Allah Ghahremani [1*], Hassan Majed Alhassan [2]

1-2. Faculty of Electrical & Computer engineering, Malek Ashtar University of Technology, Tehran

*Tehran Province, Tehran, Lavizan, Babaei Hwy

Email: *ghahremani@mut.ac.ir

This paper presents a new Modified Predictive Kalman Filter (MPKF). To solve the problem of a strap-down inertial navigation system (SINS) self-alignment process that the standard Kalman filters cannot give the optimal solution when the system model and stochastic information are unknown accurately. The proposed algorithm is applied to SINS in the initial alignment process with a large misalignment heading angle. The filter is based on the idea of an accurate predictive filter that applies n-steps ahead of prediction of the SINS model errors to effectively enhance the corrections of the current information residual error on the system. Firstly, the formulations of a novel predictive filter and a fine alignment algorithm for SINS are presented. Secondly, the vehicle results demonstrate the superior performance of the proposed method, in which the MPKF algorithm is less sensitive to uncertainty. It performs a faster and more accurate estimation of SINS' initial orientation angles compared to the conventional EKF method.

Keywords: *Modified Predictive Kalman Filter (MPKF), Self-Alignment, Strap-down Inertial Navigation System (SINS), Large Heading Angle.*

Nomenclature

$\delta(.)$ The symbol of perturbation error.

$\frac{\partial(.)}{\partial(.)}$ The symbol of The partial derivative.

$\mathbf{v}^n$ The vector of velocity in navigation frame.

v_E, v_N, v_D The East, North, and Down components of velocity.

$\boldsymbol{\varepsilon}^n$ Vector of attitude misalignment angles in navigation frame.

$\mathbf{C}_b^n$ The transformation matrix from the body to navigation frame

$\mathbf{f}^b$ The vector of accelerometers output.

$\delta\mathbf{f}^b$ The vector of accelerometers biases.

$\mathbf{f}^n$ The vector of specific force in navigation frame.

$\boldsymbol{\omega}_{in}^n$ The vector of angular velocity of navigation frame relative to inertial frame.

$\boldsymbol{\omega}_{ib}^b$ The vector of gyroscopes output.

$\delta\boldsymbol{\omega}_{ib}^b$ The vector of gyroscopes drift.

$\boldsymbol{\omega}_{ie}^n$ The vector of the earth rate in navigation frame.

$\boldsymbol{\omega}_{en}^n$ The vector of angular velocity of navigation frame relative to inertial frame

$\mathbf{g}^n$ The gravity vector represented in navigation frame.

φ The latitude angle.

r The earth radius.

θ, ϕ, ψ The Euler pitch, roll and yaw angles.

$\varepsilon_E, \varepsilon_N, \varepsilon_D$ The East, North, and Down components of misalignment angle (pitch).

1. PhD Candidate
2. Associate Professor (Corresponding Authore)

Received Date: 09 Feb. 2021
Accepted Date: 06 Nov. 2021

$\Delta\omega_N$, $\Delta\omega_E, \Delta\omega_D$	The East, North, and Down components of gyroscope drifts.
$\Delta f_N, \Delta f_E$	The North and East accelerometer biases.
$\mathbf{y}$	The measurement vector.
$\mathbf{x}$	The state vector.
$\mathbf{H}$	The measurement matrix.
υ	The measurement noise.
$\mathbf{x}_{10\times1}^{EKF}$	The state vectors with dimension 10 for EKF filter.
$\mathbf{F}_{10\times10}^{EKF}$	The state matrix representation for EKF.
$\mathbf{d}$	The model error (gyroscopes and accelerometers residual biases)
$\mathbf{d}_k^*$	The optimal model error predicted by MPKF algorithm.
$\mathbf{D}_{k,p}$	The vector of the predicted model error within the *p-1* prediction horizon.
$\mathbf{D}_{k,p}^*$	The optimal vector of the predicted model error within the *p-1* prediction horizon.
$\mathbf{X}_{k+1,p}$	The state vector of future predictions up to a horizon *p*.
$\mathbf{J}_{k+1}$	The performance function in step $k+1$.
$\mathbf{F}_x$	The extended state matrix of future predictions up to a horizon p
$\mathbf{G}_D$	The extended sensitivity model error matrix

Introduction

The initial alignment of a strap-down inertial navigation system (SINS) affects the navigation performance of the SINS directly. However, an accurate alignment must be required before the start of navigation. Otherwise, it will directly degrade the navigation accuracy [1]. Additionally, alignment accuracy and alignment time are two primary criteria that affect the self-alignment performance. Usually, the working environment of SINS is noisy, the initial misalignment angles are expected to be large, and the noise isn't Gaussian white noise (the noise characteristics of gyroscope and accelerometer). Moreover, the influences on the heading estimation will be incorrect because of its incomplete observation. In this case, the traditional Kalman filter estimation makes inaccurate results and sometimes leads to filter divergence. Consequently, estimating a large heading angle is a challenge for the recent research.

To achieve the above deficiencies, many researchers and scholars are dedicating themselves to further researching and realizing different methods to solve the self-alignment problem. Research is mainly divided into two regards; the research on a nonlinear model and the research on nonlinear filtering [12-16]. Remarkable research on a nonlinear model can be summarized as follows; a modified error model of SINS for the initial alignment process was performed under marine mooring conditions [1], while an algorithm to automatically estimate large misalignment angles was suggested in [2] and a fast alignment method was proposed based on the attitude matrix decomposition [3]. Some studies researched the alignment of SINS aided by global positioning systems (GPS) [4] or aided by gimbaled INS [5], to provide better conditions for the SINS error observability. Nevertheless, most of the methods stated previously suffer from the estimation accuracy of the heading misalignment and the big alignment time or the alignment problem is not achieved without other sensors.

In the literature, to reduce the computational complexity for the self-alignment process, a method based on the attitude determination technique was presented in [6, 7]. Several nonlinear filtering methods were applied to the initial alignment process, amongst the commonly-used methods there is the extended Kalman filter (EKF), unscented Kalman filter (UKF) [8], particle filter (PF), fading cubature Kalman filter [9], and cubature Kalman filter (CKF) [10]. An incremental predictive filter (IPF) was applied to the alignment of SINS [11]. However, the IPF filter assumes that the reference heading angle is available, and the system is time-invariant. A remarkable initial alignment method for a stable platform is stated in [17]. Most of the previous methods require a large amount of computation, the heading accuracy is generally only within a few degrees, and the covariance can diverge with respect to the SINS uncompensated modeling error.

Model predictive filtering (MPF) [18], is a real-time filter method to estimate the model error of the system. It has developed rapidly [19-21]. Unlike the Kalman filter, a predictive filter assumes a colored noise [22]. The applications of the MPF have been reported in various fields such as navigation and attitude determination [23, 24]. The conventional predictive filter, due to the use of Lie derivatives in its formulation [25], has a very complex mathematical algorithm. Despite of the advantages of the conventional predictive filter, its complexity makes so much trouble in understanding the algorithm and makes the design of the predictive filter a very time-consuming and inflexible process [16]. In fact, with minimal

changes in the dimensions of the model error vector or the model-error distributer matrix during the design process, the filter designer must recalculate all Lie derivatives. This drawback limits the widespread utilization of MPF seriously and leads to not using its advantages by engineers. Because of the high-level noise from the MEMS inertial sensors, MIMU self-alignment is generally considered impossible, and other sensors are often necessary to provide initial heading information. In recent years, many studies have begun to focus on using a MEMS north seeking. One of these papers [26] proposed to use a MEMS gyro and accelerometer to achieve a one-degree northing accuracy. The high-precision tuning fork MEMS gyroscope can achieve a north-seeking accuracy of four milli-radians in 5 min [27]. To achieve such a high north-seeking accuracy using MEMS gyros is very attractive. However, current north seeking experiments have been conducted on a static base, which limits the range of MEMS-IMU application, and can be improved by fusing gyro and accelerometer data with complementary filters [28]. However, without other aiding sensors, this algorithm cannot provide the heading information. The self-alignment of MEMS-IMU is generally considered impossible, and other sensors are often necessary to provide the initial heading information. In addition, the traditional gyro-compassing algorithm is no longer applicable for MEMS-IMU on stationary bases [12]. This study proposes to estimate the model error of the MEMS IMU (gyroscopes and accelerometers biases) to suppress the bias effect on the heading error, and then the use of online iterative filtering to achieve the self-alignment of the MEMS-IMU.
This paper introduces a modified predictive Kalman filter MPKF for SINS accurate self-alignment process (Fig.1). The goal is to reduce the effect of initial alignment errors and to increase the robust performance of the alignment process against model uncertainty and the outer disturbances. The MPKF is an approach based on optimization of a cost function to predict the SINS model error, which uses predicted n-step ahead of model error with unknown time-varying noise statistics to compensate for model errors [29]. Figure 1 shows the block diagram of the proposed algorithm. The performance of the proposed method is validated with a vehicle test, under the condition that the base is disturbed. The results demonstrate that MPKF performs a faster convergence and a more accurate estimation of the heading angle compared with the conventional EKF method.

This paper covers four main parts. Part II introduces the fundamental knowledge about the initial alignment techniques, and it presents the new state-space variables for MPKF. Part III describes the MPKF formulation and its specific algorithm. The MPKF performance will be compared with the EKF, and the results of a vehicle test will be interpreted in Part VI. Finally, Part V carries the conclusion of the research.

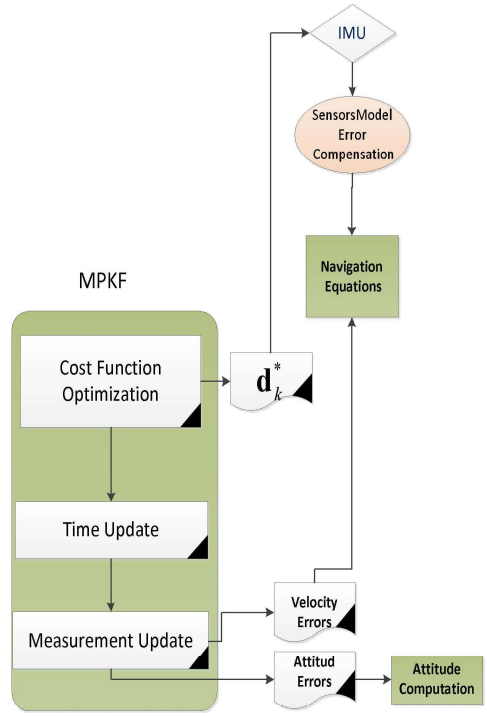

Fig.1. the block diagram of the proposed algorithm.

SINS Self-Alignment

The main purpose of the self-alignment process of SINS is to obtain the initial coordinate transformation matrix between the vehicle frame and the local navigation frame (North axis, East axis, and Down axis, that is NED) without any external aids. Traditionally, for the low-cost SINS, due to the low signal-to-noise ratio of the gyroscope, the angular rate of the earth's rotation is mixed with gyro noise, and this method is no longer applicable. Accordingly, the output of the accelerometer calculates the initial horizontal attitude angle directly, while the initial heading angle is uncertain. In other words, the alignment accuracy is significantly reduced when the disturbance is strong with a large heading misalignment angle.

For the IMUs whose bias and noise levels are smaller than the value of the Earth's rotation rate, such as navigation-grade and tactical grade IMUs including the ADIS16488A (see Table 1) , the analytic coarse alignment method followed by the fine alignment can be applied to estimate the IMU's attitude information. The coarse alignment can be calculated using the averaged data in the stationary mode. So, the analytical coarse alignment yields averaged attitude. Since the instantaneous attitude of an IMU is continuously changing by outer disturbances, the fine alignment technique is needed. The fine alignment is to estimate the attitude of an IMU with higher accuracy in time. For automotive-grade, and consumer-grade IMUs, the external heading measurements using magnetic compasses or velocity matching alignment technique are usually used.

Table 1 : Specifications for different grades of IMU [29].

Performance	CEP rate (Km/h)	Gyros (deg/h)	Accelerometers (g)
Strategic grade(<)	0.2	0.001	10-4
Navigation grade	2	0.01	10-3
Tactical grade(>)	20	0.1-10	10-2
Automotive	120	10-200	1.2
Consumer	180	>360	2.4

The gyroscope bias level of IMU ADIS16488A is rated at 5°/h, which can cause a 11.6° initial heading error. Hence, the estimation of gyroscope biases plays a significant role for tactical-grade IMUs. Figure 2 shows the value of the second term on the right hand side of equation (13) for some gyroscope bias values at latitude 35.789°. The heading error would be about 11.6°, if the gyroscope bias was 5°/h. If the bias is not estimated correctly in the fine alignment, the heading error would still remain even after filtering.

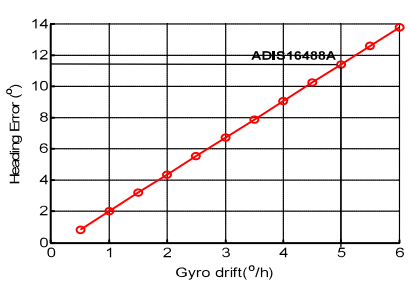

Fig.2. Coarse alignment error for ADIS16488A

In this paper, the proposed Modified Predictive Kalman Filter (MPKF) is designed to predict and to compensate for the model error in each step. Hence, the proposed algorithm performs closed-loop filtering, which combines the coarse and the fine alignment processes. At first, the analytical coarse alignment process is used to calculate the initial transformation matrix using two non-collinear vectors; the acceleration vector of gravity and the vector of the earth's rotation angular velocity. Then, the fine alignment process is adopted by linearization about the given alignment angles (from the coarse alignment), and by using the MPKF to predict and to compensate for model error. Therefore, it is better enough for fine alignment, since compensation for the disturbances is also provided.

Attitude Error Equation

From [30-32], the SINS attitude error equation can be obtained as follows:

$$\dot{\boldsymbol{\varepsilon}}^n = -\left[\boldsymbol{\omega}_{in}^n \times\right]\boldsymbol{\varepsilon}^n + \frac{\partial \omega_{in}^n}{\partial v^n}\delta \mathbf{v}^n + \frac{\partial \omega_{in}^n}{\partial r^n}\delta \mathbf{r}^n - \mathbf{C}_b^n \delta \boldsymbol{\omega}_{ib}^b \tag{1}$$

The SINS is assumed fixed without any motion. Therefore, $\boldsymbol{\omega}_{en}^n = 0$, then:

$$\dot{\boldsymbol{\varepsilon}}^n = -\left[\boldsymbol{\omega}_{in}^n \times\right]\boldsymbol{\varepsilon}^n + \delta\boldsymbol{\omega}_{in}^n - \mathbf{C}_b^n \delta \boldsymbol{\omega}_{ib}^b \tag{2}$$

Where:

$$\boldsymbol{\omega}_{in}^n = \begin{bmatrix} \frac{v_E}{r} + \omega_e \cos\varphi \\ -\frac{v_N}{r} \\ -\frac{v_E \tan\varphi}{r} - \omega_e \sin\varphi \end{bmatrix} \tag{3}$$

$$\delta\boldsymbol{\omega}_{in}^n = \left[\frac{\delta v_E}{r}, \quad \frac{-\delta v_N}{r}, \quad \frac{-\delta v_E}{r}\tan\varphi\right]^T \tag{4}$$

It is assumed that $\mathbf{C}_b^n \delta \boldsymbol{\omega}_{ib}^b$ as gyro biases $\Delta\boldsymbol{\omega}$ vector of navigation frame. The dynamics of these biases are expressed, for the EKF algorithm, as random constants $\Delta\dot{\boldsymbol{\omega}} = 0$, while, in the MPKF algorithm, $\Delta\boldsymbol{\omega}$ defines the unknown gyroscope model error.

Velcocity Error Equation

In the navigation frame, dynamics of the velocity errors of SINS [30-32] are given by:

$$\begin{aligned}\delta\dot{\mathbf{v}}^n &= -(2\delta\boldsymbol{\omega}_{ie}^n + \delta\boldsymbol{\omega}_{en}^n)\times\mathbf{v}^n + \delta\mathbf{g}^n \\ &\quad -(2\boldsymbol{\omega}_{ie}^n + \boldsymbol{\omega}_{en}^n)\times\delta\mathbf{v}^n - \boldsymbol{\varepsilon}^n\times\mathbf{f}^n + \mathbf{C}_b^n\delta\mathbf{f}^b\end{aligned} \tag{5}$$

$\delta\mathbf{f}^b$ is the accelerometer error, and $\delta\mathbf{g}^n$ the gravity error term. For static alignment, the vertical velocity error can be negligible ($\delta\mathbf{v}_D = 0$). Therefore, the dynamics of the velocity errors can be formulated as:

$$\delta\dot{\mathbf{v}}^n = -2\boldsymbol{\omega}_{ie}^n\times\delta\mathbf{v}^n - \boldsymbol{\varepsilon}^n\times\mathbf{f}^n + \mathbf{C}_b^n\delta\mathbf{f}^b \tag{6}$$

Initial Alignment Error Model

The state equation of the initial alignment filtering model can be retrieved from equation (2) and (6). Hence:

$$\begin{aligned}\dot{\varepsilon}_N &= -\omega_e\sin\varphi\varepsilon_E + \delta v_E/r - \Delta\omega_N \\ \dot{\varepsilon}_E &= +\omega_e\sin\varphi\varepsilon_N + \omega_e\cos\varphi\varepsilon_D - \delta v_N/r - \Delta\omega_E \\ \dot{\varepsilon}_D &= -\omega_e\cos\varphi\varepsilon_E - \delta v_E\tan\varphi/r - \Delta\omega_D \\ \delta\dot{v}_N^n &= -2\omega_e\sin\varphi\delta v_E - g\varepsilon_E + \Delta f_N \\ \delta\dot{v}_E^n &= +2\omega_e\sin\varphi\delta v_N + g\varepsilon_N + \Delta f_E\end{aligned} \tag{7}$$

Coarse Alignment

In the coarse-alignment process, two non-collinear vectors are adopted, the local gravity vector, and the earth rate vector.

$$\mathbf{g}^n = \begin{bmatrix}0 & 0 & g\end{bmatrix}^T \tag{8}$$

$$\boldsymbol{\omega}_e^n = \begin{bmatrix}\omega_e\cos\varphi & 0 & -\omega_e\sin\varphi\end{bmatrix}^T \tag{9}$$

The components of these vectors along with the NED frame, g and ω_e are the magnitude of the local gravity and the earth rate, respectively, and φ is the local geodetic latitude. The following equation is used to calculate the transformation matrix $\mathbf{C}_n^b$

$$\mathbf{C}_b^n = \begin{bmatrix}\mathbf{g}^{nT} \\ \boldsymbol{\omega}_e^{nT} \\ \left[\mathbf{g}^n\times\boldsymbol{\omega}_e^n\right]^T\end{bmatrix}^{-1}\begin{bmatrix}\mathbf{f}^{bT} \\ \boldsymbol{\omega}_{ib}^{b\,T} \\ \left[\mathbf{f}^b\times\boldsymbol{\omega}_{ib}^b\right]^T\end{bmatrix} \tag{10}$$

The resulted alignment matrix is as follows:

$$\mathbf{C}_b^n = \begin{bmatrix}\frac{-\tan\varphi}{g} & \frac{1}{\omega_e\cos\varphi} & 0 \\ 0 & 0 & \frac{-1}{g\omega_e\cos\varphi} \\ \frac{-1}{g} & 0 & 0\end{bmatrix}\begin{bmatrix}\mathbf{f}^{bT} \\ \boldsymbol{\omega}_{ib}^{b\,T} \\ \left[\mathbf{f}^b\times\boldsymbol{\omega}_{ib}^b\right]^T\end{bmatrix} \tag{11}$$

The Euler angles are calculated from $\mathbf{C}_b^n$ as:

$$\begin{aligned}\theta &= -\tan^{-1}(c_{31}/\sqrt{1-c_{31}^2}) \\ \phi &= \text{atan2}(c_{32},c_{33}), \\ \psi &= \text{atan2}(c_{21},c_{11}).\end{aligned} \tag{12}$$

This method is based on an idealization in which there are no accelerometer and gyro errors (and no deflection of the vertical vector). In fact, both accelerometer and gyro output data have errors. Also, even though the vehicle is stationary, it is not rigidly fixed to the earth and motions due to disturbances cause incorrect accelerometer and gyro outputs. In general, the initial errors $\varepsilon_N, \varepsilon_E, \varepsilon_D$ depend on the uncertainties in measurements of accelerations and rates by the inertial sensors and can be easily deduced to be governed by the following equations:

$$\begin{aligned}\varepsilon_N &= \frac{\Delta f_E}{g} \\ \varepsilon_E &= \frac{1}{2}\left(-\frac{\Delta f_N}{g} + \frac{\Delta f_D}{g}\tan\varphi - \frac{\Delta\omega_D}{\omega_e}\sec\varphi\right) \\ \varepsilon_D &= \frac{1}{2}\left(-\frac{\Delta f_E}{g}\tan\varphi + \frac{\Delta\omega_E}{\omega_e}\sec\varphi\right)\end{aligned} \tag{13}$$

Mainly, the heading accuracy is affected by the east gyro and accelerometer errors, if bias is not estimated precisely in the fine alignment, the heading error remains after filtering.

The Proposed Coarse Alignment

The traditional formula of the estimated heading angle $\hat{\psi}$ that is presented in equation (12) contains the output of three gyroscopes. The proposed method is similar to the traditional method, but it has the less computational operation. It uses the horizontal body frame compensated measurements of the accelerometers $\mathbf{f}^b$ and the gyros $\boldsymbol{\omega}_{ib}^b$. The three Euler angles can be determined by the following equations:

$$\hat{\theta} = \sin^{-1}(\hat{c}_{31}) = \sin^{-1}(\frac{-\mathbf{f}_N^b}{g})$$

$$\hat{\phi} = \sin^{-1}(\frac{\hat{c}_{32}}{\cos\hat{\theta}}) = \sin^{-1}(\frac{-\mathbf{f}_E^b}{g\sqrt{1-\sin^2\hat{\theta}}})$$

$$\cos\hat{\psi} = \frac{\hat{c}_{11}}{\cos\theta} = \frac{\boldsymbol{\omega}_{ibN}^b - \omega_e \sin\varphi \sin\hat{\theta}}{\omega_e \cos\varphi \cos\hat{\theta}}$$

$$\sin\hat{\psi} = \frac{-\boldsymbol{\omega}_{ibE}^b - \omega_e \sin\varphi \sin\hat{\phi}\cos\hat{\theta}}{\omega_e \cos\varphi \cos\hat{\phi}} + \sin\hat{\theta}\tan\hat{\phi}\cos\hat{\psi}$$

$$\hat{\psi} = \tan^{-1}(\frac{\sin\hat{\psi}}{\cos\hat{\psi}})$$

Real Time Calculation

The horizontal accelerometers outputs are collected and the average value is calculated according to the following formula:

$$\overline{\mathbf{f}}_i^b(n) = \overline{\mathbf{f}}_i^b(n-1) + \frac{\mathbf{f}_i^b(n) - \overline{\mathbf{f}}_i^b(n-1)}{n}$$

Where, $i = N, E \quad n = 2,3,\cdots$. The initial pitch angle and the roll angle are calculated at the current time as:

$$\theta(n) = \sin^{-1}(\frac{\overline{\mathbf{f}}_E^b(n)}{g}), \qquad \phi(n) = -\sin^{-1}(\frac{\overline{\mathbf{f}}_N^b(n)}{g})$$

Where, $\overline{\mathbf{f}}_i^b(n)$ is the average output value of the previous n data, $\overline{\mathbf{f}}_i^b(n-1)$ is the average output value of the previous *n-1* data, $\mathbf{f}_i^b(n)$ is the current output value. The horizontal gyroscopes output are collected and the average value is calculated according to the following formula:

$$\overline{\boldsymbol{\omega}}_{ibj}^b(n) = \overline{\boldsymbol{\omega}}_{ibj}^b(n-1) + \frac{\boldsymbol{\omega}_{ibj}^b(n) - \overline{\boldsymbol{\omega}}_{ibj}^b(n-1)}{n}$$

Where, $i = N, E \quad n = 2,3,\cdots$.

Fine Alignment

The coarse alignment process can provide small angles deviations between the indicated and the ideal alignments. These deviations result from the model errors and the systematic errors in the sensors that cannot be estimated. Therefore, the alignment accuracy is resolved to the gyro drift and accelerometer bias. That is, the model errors decrease alignment accuracy or even lead to divergence of the filter. In this paper, to increase the alignment accuracy, the fine alignment process will be mixed to coarse alignment to improve the estimated initial alignment matrix by applying the proposed MPKF filter, which predicts the model errors.

Choice of State Space Variable

Frequently, in static alignment, the position and the vertical velocity errors are ignored. Therefore, the level velocity errors, misalignment angles, the constant accelerometer biases, and the constant gyro drifts are preferred as the state variables for EKF filter. In this case, the state vector for the system error model is specified by:

$$\mathbf{x}_{10\times1}^{EKF} = \begin{bmatrix} \varepsilon_N, \varepsilon_E, \varepsilon_D, \delta v_N, \delta v_E, ... \\ \Delta\omega_N, \Delta\omega_E, \Delta\omega_D, \Delta f_N, \Delta f_E \end{bmatrix}^T \tag{14}$$

Then,

$$\dot{\mathbf{x}}_{10\times1}^{EKF} = \mathbf{F}_{10\times10}^{EKF}\mathbf{x}_{10\times1}^{EKF} \tag{15}$$

The combined deterministic and stochastic model error state vector in the navigation frame is selected as the state space for MPKF. It takes the following form:

$$\dot{\mathbf{x}}_{5\times1}^{MPKF} = \mathbf{F}_{5\times5}^{MPKF}\mathbf{x}_{5\times1}^{MPKF} + \mathbf{d}_{5\times1} \tag{16}$$

where:

$$\mathbf{x}_{5\times1}^{MPKF} = \begin{bmatrix} \varepsilon_N & \varepsilon_E & \varepsilon_D & \delta v_N & \delta v_E \end{bmatrix}^T \tag{17}$$

Where $\varepsilon_N, \varepsilon_E, \varepsilon_D$ are the misalignment errors for the transformation between the b-frame and the navigation frame. δv_N and δv_E are the north and the east velocity errors. The vector $\mathbf{d}$ represents the random part of the error model (gyroscopes and accelerometers residual biases). The state vector of the system error model is defined as:

$$\mathbf{d}_{5\times1} = \begin{bmatrix} \Delta\omega_N & \Delta\omega_E & \Delta\omega_D & \Delta f_N & \Delta f_E \end{bmatrix}^T \tag{18}$$

Measurment

The pseudo measurements $v_N = v_E = 0$ can be used as a direct measure of the errors δv_N, δv_E, each denoting the difference between the velocity indicated by the system and the visible (Earth-referenced) velocity of the system (ideally zero, if the vehicle is stationary).The heading indicated by the system can be extracted from the computed $\mathbf{C}_b^n$:

$$\psi = \text{atan2}(c_{21}, c_{11}) \tag{19}$$

Moreover, the fact that the heading error is not completely observable is widely accepted. The pseudo measurement of the heading angle is the

difference between the heading indicated by the SINS and the heading estimated by the filter. The linear relationship between observations and states is given by:

$$\mathbf{y} = \mathbf{H}\mathbf{x} + \boldsymbol{\upsilon} \tag{20}$$

Where $\boldsymbol{\upsilon} \sim N(\mathbf{0}, \mathbf{R})$, the matrix $\mathbf{H}$ for EKF is given by:

$$\mathbf{H}_{3\times10}^{EKF} = \begin{bmatrix} 0 & 0 & 0 & 1 & 0 & \\ 0 & 0 & 0 & 0 & 1 & \mathbf{0}_{3\times5} \\ 0 & 0 & 1 & 0 & 0 & \end{bmatrix} \tag{21}$$

The matrix $\mathbf{H}$ for MPKF is as follows:

$$\mathbf{H}_{3\times5}^{MPKF} = \begin{bmatrix} 0 & 0 & 0 & 1 & 0 \\ 0 & 0 & 0 & 0 & 1 \\ 0 & 0 & 1 & 0 & 0 \end{bmatrix} \tag{22}$$

The covariance matrix of measurements is:

$$\mathbf{R} = diag\left[\sigma_{vel}^2 \quad \sigma_{vel}^2 \quad \sigma_{azimuth}^2\right]\Delta t \tag{23}$$

With σ_{vel} and $\sigma_{azimuth}$, representing the standard deviations of the velocity and azimuth observations.

Modified Predictive Kaman Filter (MPKF)

The Modified Predictive Kaman Filter (MPKF) indicates an estimation methodology that calculates optimal model errors based on a model of a dynamical system and its predicted future evolution. The idea of the MPKF strategy has come from the duality between the concept of incremental predictive control [16] and the estimation theory. MPKF is designed as a real-time optimization problem that repeatedly predicts model errors by minimizing a quadratic cost function.

The estimation part, shown in Fig.3, uses past data to estimate the current state. Kalman filter achieves exactly this for linear models subject to process noise and measurement noise. The prediction part in Fig.1 estimates a trajectory of the model error such that a predicted output tracks a reference objective as well as possible. Then, only the first part of the predicted model error must be implemented. Next, the method repeated at the next sampling time by moving the horizon of prediction. It is important to realize that this repeated optimization procedure enables the MPKF to decrease the model uncertainties and external disturbances.

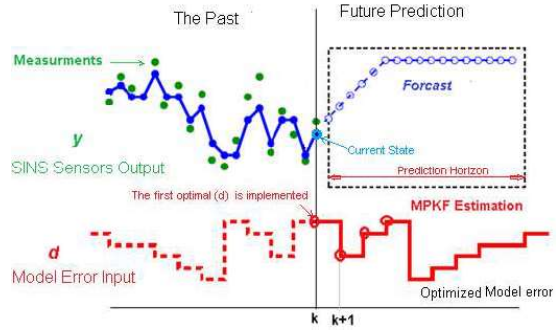

Fig.3. Modified predictive estimation principle.

The uncertainty of SINS model errors is defined as the deviations of sensors deterministic errors from the SINS calibration values; including bias, scale factor, and misalignment angles of the inertial sensors.

State Space Model

The discrete form of the nonlinear state equation (7) of the initial alignment model and the observation equation can be formulated as:

$$\begin{aligned} \mathbf{X}_{k+1} &= f(\mathbf{X}_k, \mathbf{d}_k) + \mathbf{w}_k \\ \mathbf{Y}_k &= h(\mathbf{X}_k) + \mathbf{v}_k \end{aligned} \tag{24}$$

Defining, $\mathbf{Q}_k$ and $\mathbf{R}_k$ as a symmetric positive semi-definite matrices that represent the covariance of the normally distributed random noises $\mathbf{w}_k$ and $\mathbf{v}_k$.

Problem Statement

The MPKF predicts the future of the model error performance. This section details how to calculate these forecasts for model error. Considering the linearized discrete-time state space of the system mode, Equation (23), this gives the one step ahead prediction as following:

$$\begin{aligned} \hat{\mathbf{x}}_{k+1/k} &= \mathbf{F}_k \hat{\mathbf{x}}_k + \mathbf{d}_k \\ \hat{\mathbf{y}}_{k+1/k} &= \mathbf{H}\,\hat{\mathbf{x}}_{k+1/k} \end{aligned} \tag{25}$$

The Equation (24) at sample k + 2 can be formed as:

$$\hat{\mathbf{x}}_{k+2/k} = \mathbf{F}_k \hat{\mathbf{x}}_{k+1/k} + \mathbf{d}_{k+1/k} \tag{26}$$

Substitute (24) into (26) to eliminate $\hat{\mathbf{x}}_{k+1/k}$

$$\begin{aligned}\hat{\mathbf{x}}_{k+2/k} &= \mathbf{F}_k^2\hat{\mathbf{x}}_k + \mathbf{F}_k\mathbf{d}_k + \mathbf{d}_{k+1/k}\\ \hat{\mathbf{y}}_{k+2/k} &= \mathbf{H}\,\hat{\mathbf{x}}_{k+2/k}\\ \hat{\mathbf{y}}_{k+2/k} &= \mathbf{H}\,\mathbf{F}_k^2\hat{\mathbf{x}}_k + \mathbf{H}\,\mathbf{F}_k\mathbf{d}_k + \mathbf{H}\,\mathbf{d}_{k+1/k}\end{aligned} \tag{27}$$

More generally by continuing this recursion to give the p-step ahead predictions as:

$$\begin{aligned}\hat{\mathbf{x}}_{k+p/k} &= \mathbf{F}_k^p\hat{\mathbf{x}}_k + \mathbf{F}_k^{p-1}\mathbf{d}_k + \cdots + \mathbf{d}_{k+p-1/k}\\ \hat{\mathbf{y}}_{k+p/k} &= \mathbf{H}\,\mathbf{F}_k^p\hat{\mathbf{x}}_k + \mathbf{H}\,\mathbf{F}_k^{p-1}\mathbf{d}_k + \cdots + \mathbf{H}\,\mathbf{d}_{k+p-1/k}\end{aligned} \tag{28}$$

Hence, the whole vector of future predictions up to a horizon p is given by Equations (29, 30).

$$\mathbf{X}_{k+1,p} = \mathbf{F}_x\hat{\mathbf{x}}_k + \mathbf{G}_D\mathbf{D}_{k,p} \tag{29}$$

$$\mathbf{Y}_{k+1,p} = \mathbf{H}\,\mathbf{F}_x\hat{\mathbf{x}}_k + \mathbf{H}\,\mathbf{G}_D\mathbf{D}_{k,p} \tag{30}$$

Where,

$$\mathbf{X}_{k+1,p} = \begin{bmatrix}\hat{\mathbf{x}}_{k+1/k}\\ \hat{\mathbf{x}}_{k+2/k}\\ \vdots\\ \hat{\mathbf{x}}_{k+p/k}\end{bmatrix};\mathbf{F}_x = \begin{bmatrix}\mathbf{F}_k\\ \mathbf{F}_k^2\\ \vdots\\ \mathbf{F}_k^p\end{bmatrix};\mathbf{D}_{k,p} = \begin{bmatrix}\mathbf{d}_k\\ \mathbf{d}_{k+1/k}\\ \vdots\\ \mathbf{d}_{k+p-1/k}\end{bmatrix}$$

$$\mathbf{G}_D = \begin{bmatrix}\mathbf{I} & \mathbf{0} & \mathbf{0} & \dots & \mathbf{0}\\ \mathbf{F}_k & \mathbf{I} & \mathbf{0} & \dots & \mathbf{0}\\ \mathbf{F}_k^2 & \mathbf{F}_k & \mathbf{I} & \dots & \mathbf{0}\\ \vdots & \vdots & \vdots & \dots & \mathbf{0}\\ \mathbf{F}_k^{p-1} & \mathbf{F}_k^{p-2} & \mathbf{F}_k^{p-3} & \dots & \mathbf{I}\end{bmatrix};\mathbf{Y}_{k+1,p} = \begin{bmatrix}\hat{\mathbf{y}}_{k+1/k}\\ \hat{\mathbf{y}}_{k+2/k}\\ \vdots\\ \hat{\mathbf{y}}_{k+p/k}\end{bmatrix} \tag{31}$$

Consequently, the predictions of future states and outputs over the prediction horizon are affine in the current state and the future model error moves, $\mathbf{H}\,\mathbf{F}_x$ is a reaction of the system output to state $\hat{\mathbf{x}}_k$, and $\mathbf{H}\,\mathbf{G}_D$ is a reaction of the system output to model error moves $\mathbf{D}_{k,p}$.

Basic Algorithm of MPKF

The MPKF manages the process model to predict the future model error over a determined prediction horizon p. At each time step, an optimization problem is solved to calculate the sequence of future model error moves. The first one of optimal model error moves is applied to the process model. At the next time step, the prediction horizon of the optimization problem is shifted forward in time, and the procedure is repeated.

Performance Criterion

The MPKF algorithm requires a cost function in its formulation to calculate the optimal solution at each sampling interval.

For the SINS self-alignment, the penalty function penalizes the weighted norm of the current innovation measurement states and the norm of the model error.

$$\begin{aligned}\mathbf{d}_k^* &= \min_{\mathbf{d}_{k,p}} \mathrm{J}_{k+1}(\mathrm{x}_{k+1}, p)\\ \mathbf{d}_k^* &= \min_{\mathbf{d}_{k,p}}(\rho\mathbf{Y}_{k+1,p}^T\mathbf{Y}_{k+1,p} + \lambda\mathbf{D}_{k,p}^T\mathbf{D}_{k,p})\end{aligned} \tag{32}$$

This implies that the filter can predict a model error that will drive the system towards the desired object. In the quadratic form of equation (32), the term $\rho\mathbf{I}$ and $\lambda\mathbf{I} \geq 0$ are both diagonal and they satisfy $\rho\mathbf{I} \geq 0, \lambda\mathbf{I} \geq 0$. With proper substitution, the cost function in Equation (32) can be simplified, respectively, as:

$$\begin{aligned}\mathbf{J}_{k+1}(\mathbf{x}_{k+1}, p) = {} & \mathbf{Y}_{k+1,p}^T\rho\mathbf{I}\mathbf{Y}_{k+1,p} + \mathbf{D}_{k,p-1}^T\lambda\mathbf{I}\mathbf{D}_{k,p-1}\\ &= \mathbf{D}_{k,p-1}^T\left[\mathbf{G}_D^T\mathbf{H}_{k+1}^T\rho\mathbf{I}\mathbf{H}_{k+1}\mathbf{G}_D + \lambda\mathbf{I}\right]\mathbf{D}_{k,p-1}\\ &+2\left[(\mathbf{H}_{k+1}\mathbf{F}_k\hat{\mathbf{x}}_k)^T\rho\mathbf{I}\mathbf{H}_{k+1}\mathbf{G}_k^d\right]\mathbf{D}_{k,p-1}\\ &+(\mathbf{H}_{k+1}\mathbf{F}_k\hat{\mathbf{x}}_k)^T\rho\mathbf{I}(\mathbf{H}_{k+1}\mathbf{F}_k\hat{\mathbf{x}}_k)\end{aligned} \tag{33}$$

The optimization problem can be solved by minimization of the cost function using least-squares formulation. Least squares allow analytical solution for an unconstrained problem and penalize larger errors more than smaller errors. The solution of this cost function can be obtained by computing the derivative of $\mathbf{J}_{k+1}(\mathbf{x}_{k+1}, p)$ and equating it to zero:

$$\frac{\partial\mathbf{J}_{k+1}(\mathbf{x}_{k+1}, p)}{\partial\mathbf{D}_{k,p}} = 0, \tag{34}$$

The solution is:

$$\mathbf{D}_{k,p}^* = -\left(\rho\left[\rho\mathbf{H}^T\mathbf{G}_D^T\mathbf{G}_D\mathbf{H} + \lambda\mathbf{I}\right]^{-1}\mathbf{H}^T\mathbf{G}_D^T\mathbf{H}\,\mathbf{F}_x\right)\hat{\mathbf{x}}_k \tag{35}$$

Defining the MPKF gain:

$$\mathbf{K}_{MPKF} = -\rho\left[\rho\mathbf{H}^T\mathbf{G}_D^T\mathbf{G}_D\mathbf{H} + \lambda\mathbf{I}\right]^{-1}\mathbf{H}^T\mathbf{G}_D^T\mathbf{H}\,\mathbf{F}_x \tag{36}$$

Then,

$$\mathbf{D}_{k,p}^* = -\mathbf{K}_{MPKF}\hat{\mathbf{x}}_k \tag{37}$$

There is optimal model error sequence $\mathbf{D}^*_{k,p-1}$ found, but only the first model error move is applied to system, that is:

$$\mathbf{d}^*_k = -[\mathbf{I} \quad 0 \quad \cdots \quad 0]^T \mathbf{K}_{MPKF} \hat{\mathbf{x}}_k \tag{38}$$

After applying the first model error move of optimal sequence to system, new output is measured and new optimal model error sequence $\mathbf{D}^*_{k+1,p}$ is computed. The simplified MPKF framework algorithm is as follows:

1-Initialization at step $k = 0$. Supposing the initial state variable and the covariance matrices are:

$$\begin{aligned} &\hat{\mathbf{x}}_0 = E[\mathbf{x}_0], \mathbf{d}_0 = \mathbf{0} \\ &\mathbf{P}_0 = E[(\mathbf{x}_0 - \hat{\mathbf{x}}_0)(\mathbf{x}_0 - \hat{\mathbf{x}}_0)^T] \\ &\mathbf{Q} = E[(\mathbf{w})(\mathbf{w})^T] \\ &\mathbf{R} = E[(\mathbf{v})(\mathbf{v})^T] \end{aligned} \tag{39}$$

2- The optimal model error is calculated as following:

$$\mathbf{d}^*_k = -[1 \quad 0 \quad \cdots \quad 0]^T \mathbf{K}_{MPF} \hat{\mathbf{x}}_k \tag{40}$$

3- Time updating:

Computing the predicted state estimate:

$$\hat{\mathbf{x}}_{k+1/k} = \mathbf{F}_k \hat{\mathbf{x}}_k + \mathbf{G}_{dk} \mathbf{d}^*_k \tag{41}$$

Computing the predicted measurement

$$\hat{\mathbf{x}}_{k+1/k} = \mathbf{F}_k \hat{\mathbf{x}}_k + \mathbf{G}_{dk} \mathbf{d}^*_k \tag{42}$$

Computing a prior covariance matrix:

$$\mathbf{P}_{k+1/k} = \mathbf{F}_k \mathbf{P}_k \mathbf{F}^T_k + \mathbf{Q}_k \tag{43}$$

Computing the Kalman gain:

$$\mathbf{K}_{k+1} = \mathbf{P}_{k+1/k} \mathbf{H}^T_{k+1} \left[\mathbf{H}_{k+1} \mathbf{P}_{k+1/k} \mathbf{H}^T_{k+1} + \mathbf{R}_{k+1} \right]^{-1} \tag{44}$$

4- Measurement updating:

Correcting the predicted estimate on the measurement:

$$\hat{\mathbf{x}}_{k+1} = \hat{\mathbf{x}}_{k+1/k} + \mathbf{K}_{k+1} \left[\mathbf{y}_{k+1} - \hat{\mathbf{y}}_{k+1/k} \right] \tag{45}$$

Computing a posterior covariance matrix:

$$\mathbf{P}_{k+1} = \left[\mathbf{I} - \mathbf{K}_{k+1} \mathbf{H}_{k+1} \right] \mathbf{P}_{k+1/k} \tag{46}$$

According to the above analysis, the SINS self-alignment using MPKF algorithm is shown in Fig.4. Here, to solve the problem of large initial heading angle error, the closed-loop MPKF algorithm is proposed. The precise alignment may be performed with a large azimuth angle error, even 180°. With this technique, the self- alignment does not need too much time (30 sec).

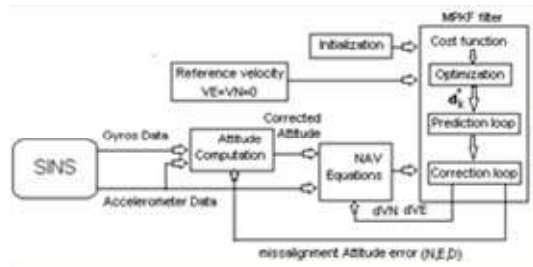

Fig.4. Modified predictive estimation principle.

Vehicle Test and Results

In this section, for experimental evaluation purpose, a real time vehicle test was performed. The performance of the EKF and MPKF will be compared and investigated.

The real-time test uses a tactical grade SINS, type AIDS16488A (Fig.5). The SINS is mounted rigidly related to the body of a stationary vehicle of accurately known longitude, latitude, and height. The raw measurements of SINS together with the orientation, velocity, and position of SINS, with respect to local level NED frame, are provided at the same rate, 200 Hz. Online data storing is executed through a serial RS-422 port on an integrated on-board computer. ADIS16488A has been used as measurement data. The main statistical features of these inertial sensors are given in Table 2.

Table.2. Specifications of inertial sensors.

Parameter	Gyroscopes	Accelerometers
Misalignment Axis	±0.05°	±0.035°
Nonlinearity	0.01%	0.1%
Bias Repeatability	±0.2°/s	±16 mg
In-Run Bias Stability	5.1°/h	0.07 mg
Random Walk	0.26°/√h	0.029 m/s/√h
Output Noise	0.135°/s	1.29 mg rms
Noise Density	0.0059°/s/√Hz	0.063 mg/√Hz

Fig.5. The hardware for test set up.

To judge the performance of the EKF and the proposed MPKF, each filter was applied to the same SINS raw data (Fig.6 and Fig.7). In this test, the output of gyroscopes and accelerometers of SINS were placed on a vehicle with the engine on (to produce some outer disturbances).

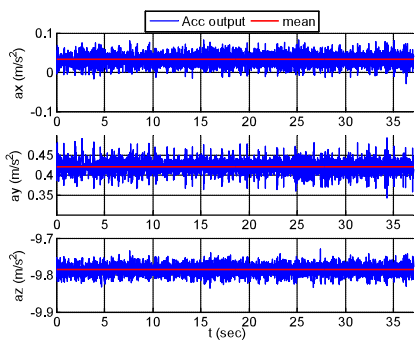

Fig.6. The ADIS16488A accelerometers output

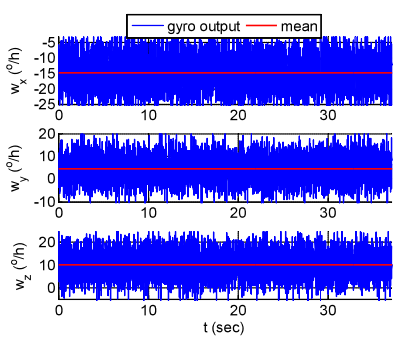

Fig.7. The ADIS16488A gyroscopes output.

Therefore ADIS16488A senses the earth rate but not accurately (see Table.3). The proposed method will predict and compensate for gyros errors.

Table.3. The raw data from gyroscopes

	Theoretical values for attitude angle Phi=35.793° and Az=175°	The mean of gyro output without compensating the roll and pitch angles and gyro drifts
Wx (°/h)	-12.15198	-14.6668
Wy (°/h)	1.063	4.4452
Wz (°/h)	8.79776	10.2715

Three different kinds of initial attitude angles are selected as follows: The levelling misalignment angles are about 3°, 7.8°, the large heading misalignment angle is about 174°. The EKF and MPKF are used to solve the above initial alignment problem, respectively. The test results are illustrated in Figs.8-12. The figures show the estimation error of Euler's angles, north and east velocity.

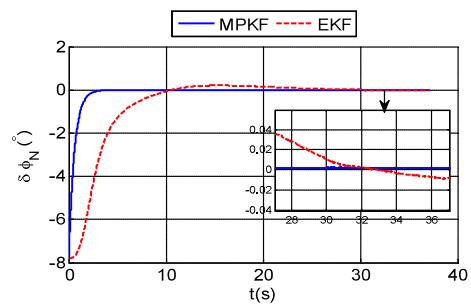

Fig.8. Estimated error of roll angle through GPKF and EKF

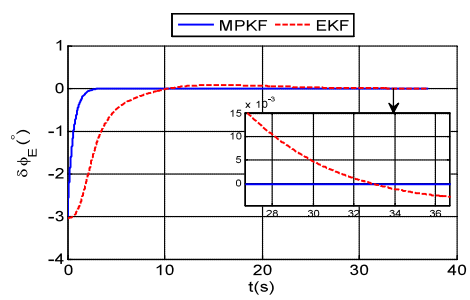

Fig.9. Estimated error of Pitch angle through GPKF and EKF

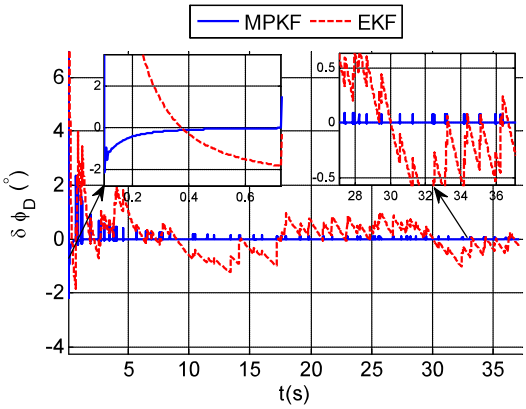

Fig.10. Estimated error of heading angle through GPKF and EKF

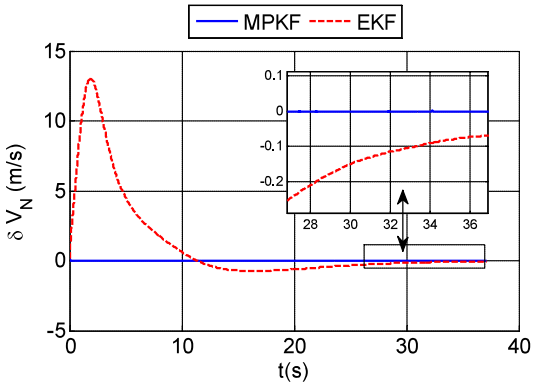

Fig.11. Estimated error of δv_N through GPKF and EKF

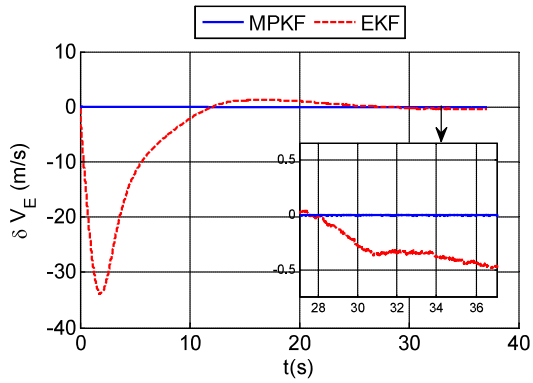

Fig.12. Estimated error of δv_E through GPKF and EKF

The estimation error of roll, pitch, and heading angles using MPKF was very accurate with respect to the estimation of EKF. The steady-state estimation error of each of roll, pitch, and heading angles are of the order of 0.11 arc. min, 0.017 arc. min and 0.059 arc. min, respectively. While the steady-state estimation error of EKF for roll, pitch, and heading angles are of the order of 0.51 arc. min, 0.18 arc. min and 17.8 arc. min, respectively. In order to explain the results of EKF and the proposed MPKF filter under disturbance error conditions more clearly, statistical results are shown in Table 4. As a result, the alignment accuracy using the MPKF is significantly higher than EKF.

Table.4. Comparison of the accuracy of estimated errors between EKF and MPKF

Error	MPKF		EKF		Std
	Mean	Steady	Mean	Steady	
ε_N **arc.min**	40.9	0.11	113.	-0.51	0.0006
ε_E **arc.min**	16.1	-0.017	44.3	-0.18	0.0006
ε_D **arc.min**	49.3	-0.059	116	-17.8	0.0217
δv_N **(m/s)**	2.7e-5	-4.4e-6	0.06	0.001	0.0002
δv_E **(m/s)**	8.3e-5	-4.4e-5	0.15	0.008	0.0002

Next, analyze the convergence speed. In Figs.8-12, the convergence speed of MPKF method is nearly the same for all variables (less than 5sec), where the convergence speeds of EKF is slower than MPKF method (more than 25sec). The MPKF filter could eliminate the effect of the inertial sensors' noise levels and model errors, the effect of bias, correlated noise, and scale factor noise. The MPKF can bind their effects, and its transient states are very smooth and are not far from the steady-state (see Fig. 10). While the EKF filter couldn't eliminate the effect of the inertial sensors noise other than the white noise.

The real test was prepared to approve the performance of the proposed MPKF for SINS self-alignment process with a large heading angle.

Fig. 13 presents that the estimated large heading angle is accurate, and the estimated error is decreased efficiently when using the MPKF filter.

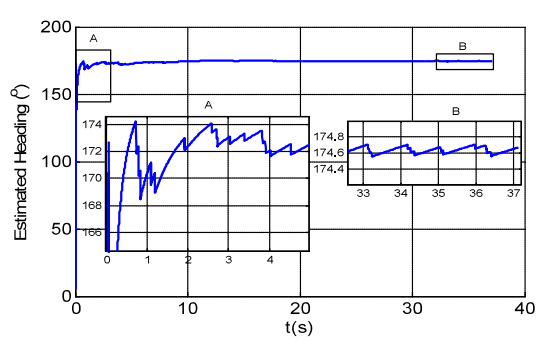

Fig.13. Estimated large heading angle by MPKF

To evaluate and validate the outcomes and claims, the time-history of covariance (Fig.14), Kalman gains (Fig.15), and model errors (Fig.16), are presented.

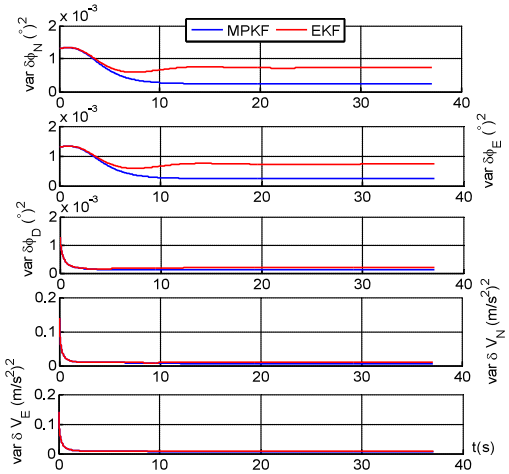

Fig.14. Estimated errors covariance.

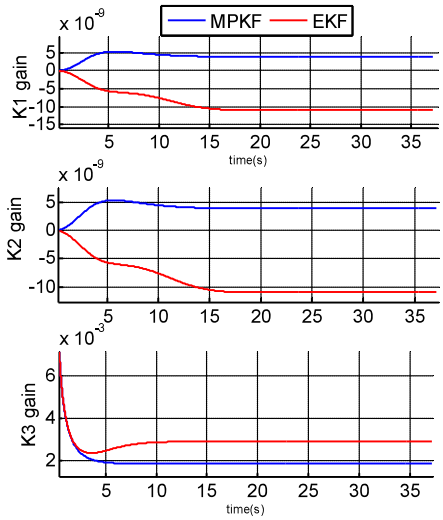

Fig.15. Kalman gains.

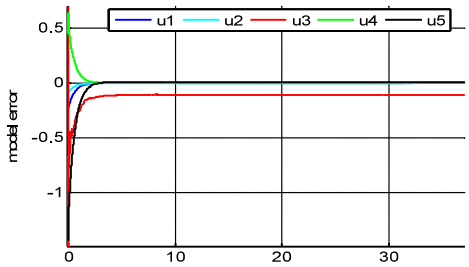

Fig.16. The estimated model errors.

In this paper, the main purpose of the self-alignment process of SINS is to obtain the initial coordinate transformation matrix between the vehicle body frame and the local navigation frame (NED) without any external aids.

Fig. 17 presents the results of the actual azimuth angle from GPS data (reference angle is 174°) when the vehicle starts moving.

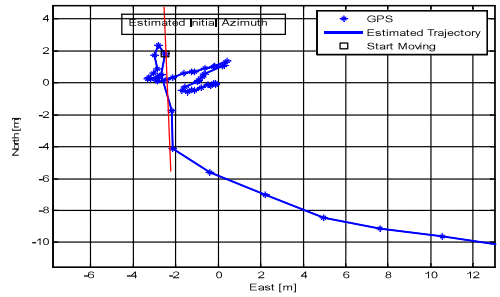

Fig.17. The starting position of static alignment and the reference data (the actual azimuth angle is 174°) when the vehicle starts moving.

The trajectory of the tested SINS is presented in Fig. 18.

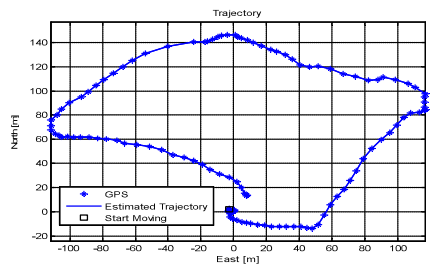

Fig.18. The vehicle trajectory.

Conclusion

In this paper, a novel self-accurate initial alignment filter named Modified Predictive Kalman Filter (MPKF) is introduced to estimate the initial alignment angles of a strap-down inertial navigation system (SINS) with a large heading angle, in the presence of model errors and outer disturbances.

The MPKF filter uses n-step ahead prediction of the SINS model errors by optimizing a quadratic cost function, to correct the current information residual error on the SINS. This leads to an accurate and fast SINS self-alignment process. The MPKF formulation is presented with a detailed closed-loop self-alignment algorithm, which combines the coarse and the fine alignment processes.

A real vehicle test is prepared to verify the performance of the proposed MPKF for SINS self-

alignment process with a large heading angle. The results demonstrate that the estimation errors of the MPKF are remarkably less than the estimation errors of the EKF because the MPKF can estimate the inertial sensors model errors more accurately, unlike the EKF.

Reference

[1] L. Chang, F. Qin, and S. Jiang, "Strapdown inertial navigation system initial alignment based on modified process model," IEEE Sensors Journal, vol. 19, no. 15, pp. 6381-6391, 2019.

[2] H. Han, J. Wang, and M. Du, "A fast SINS initial alignment method based on RTS forward and backward resolution," Journal of Sensors, vol. 2017, 2017.

[3] F. O. Silva, E. M. Hemerly, and W. C. Leite Filho, "On the error state selection for stationary SINS alignment and calibration Kalman filters–part I: Estimation algorithms," Aerospace Science and Technology, vol. 61, pp. 45-56, 2017.

[4] F. Silva, E. Hemerly, and W. Leite Filho, "On the error state selection for stationary SINS alignment and calibration Kalman filters—Part II: Observability/estimability analysis," Sensors, vol. 17, no. 3, p. 439, 2017.

[5] Y. Zhang, L. Luo, T. Fang, N. Li, and G. Wang, "An improved coarse alignment algorithm for odometer-aided SINS based on the optimization design method," Sensors, vol. 18, no. 1, p. 195, 2018.

[6] S. Guo, M. Wu, J. Xu, and F. Zha, "b-frame velocity aided coarse alignment method for dynamic SINS," IET Radar, Sonar & Navigation, vol. 12, no. 8, pp. 833-838, 2018.

[7] M. Mu and L. Zhao, "A GNSS/INS-integrated system for an arbitrarily mounted land vehicle navigation device," GPS Solutions, vol. 23, no. 4, p. 112, 2019.

[8] B. Xu, L. Wang, T. Duan, K. Jin, and J. Zhang, "A fast in-motion alignment based on inertial frame and reverse navigation," in 2020 IEEE/ION Position, Location and Navigation Symposium (PLANS), 2020, pp. 704-713: IEEE.

[9] G. Emel'yantsev, A. Stepanov, and B. Blazhnov, "Initial Alignment of SINS Measuring Unit and Estimation of Its Errors Using Satellite Phase Measurements," Gyroscopy and Navigation, vol. 10, no. 2, pp. 62-69, 2019.

[10] L. Vodicheva, L. Belsky, Y. Parysheva, and E. Koksharov, "Improving the Accuracy of Initial Alignment of Strapdown INS with the Help of Gimballed INS," in 2020 27th Saint Petersburg International Conference on Integrated Navigation Systems (ICINS), 2020, pp. 1-4: IEEE.

[11] H. Jameian, B. Safarinejadian, and M. Shasadeghi, "A robust and fast self-alignment method for strapdown inertial navigation system in rough sea conditions," Ocean Engineering, vol. 187, p. 106196, 2019.

[12] H. Xing, Z. Chen, C. Wang, M. Guo, and R. Zhang, "Quaternion-based Complementary Filter for Aiding in the Self-Alignment of the MEMS IMU," in 2019 IEEE International Symposium on Inertial Sensors and Systems (INERTIAL), 2019, pp. 1-4: IEEE.

[13] F. Zha, S. Guo, and F. Li, "An improved nonlinear filter based on adaptive fading factor applied in alignment of SINS," Optik, vol. 184, pp. 165-176, 2019.

[14] S. Guo, L. Chang, Y. Li, and Y. Sun, "Robust fading cubature Kalman filter and its application in initial alignment of SINS," Optik, vol. 202, p. 163593, 2020.

[15] T. Zhang, J. Wang, B. Jin, and Y. Li, "Application of improved fifth-degree cubature Kalman filter in the nonlinear initial alignment of strapdown inertial navigation system," Review of Scientific Instruments, vol. 90, no. 1, p. 015111, 2019.

[16] M. Fathi, N. Ghahramani, M. A. Shahi Ashtiani, A. Mohammadi, and M. Fallah, "Incremental predictive Kalman filter for alignment of inertial navigation system," Proceedings of the Institution of Mechanical Engineers, Part G: Journal of Aerospace Engineering, p. 0954410018794324, 2018.

[17] M.-A. Massoumnia and R. Rezaii-Far, "Stable platform initial alignment using state feedback controllers," in [Proceedings 1992] The First IEEE Conference on Control Applications, 1992, pp. 326-329: IEEE.

[18] J. L. Crassidis and F. L. Markley, "Predictive filtering for nonlinear systems," Journal of Guidance, Control, and Dynamics, vol. 20, no. 3, pp. 566-572, 1997.

[19] H. Odéen and D. Parker, "Dynamical model parameter adjustments in model predictive filtering MR thermometry," Journal of therapeutic ultrasound, vol. 3, no. 1, p. P31, 2015.

[20] W. Qiuying, Z. Minghui, G. Zheng, and W. Hui, "Integrated navigation method using marine inertial navigation system and star sensor based on model predictive filtering," in 2018 IEEE/ION Position, Location and Navigation Symposium (PLANS), 2018, pp. 850-857: IEEE.

[21] L. Zhang, S. Qian, S. Zhang, and H. Cai, "Federated nonlinear predictive filtering for the gyroless attitude determination system," Advances in Space Research, vol. 58, no. 9, pp. 1671-1681, 2016.

[22] A. Zenere and M. Zorzi, "Model predictive control meets robust Kalman filtering," IFAC-PapersOnLine, vol. 50, no. 1, pp. 3774-3779, 2017.

[23] L. Cao, X. Chen, and A. K. Misra, "A novel unscented predictive filter for relative position and attitude estimation of satellite formation," Acta Astronautica, vol. 112, pp. 140-157, 2015.

[24] L. Cao and H. Li, "Norm-constrained predictive filtering for attitude estimation," Proceedings of the Institution of Mechanical Engineers, Part G: Journal of Aerospace Engineering, vol. 230, no. 10, pp. 2000-2006, 2016.

[25] J. Fang and X. Gong, "Predictive iterated Kalman filter for INS/GPS integration and its application to SAR motion compensation," IEEE Transactions on Instrumentation and Measurement, vol. 59, no. 4, pp. 909-915, 2009.

[26] N. H. Ariffin, I. R. I. Zakaria, N. Arsad, A. A. A. Bakar, B. Bais, and M. S. D. Zan, "Autonomous MEMS Gyroscope and Accelerometer for North Finding System," Journal of Telecommunication, Electronic and Computer Engineering (JTEC), vol. 10, no. 1-2, pp. 13-17, 2018.

[27] B. Johnson et al., "Tuning fork MEMS gyroscope for precision northfinding," in 2015 DGON Inertial Sensors and Systems Symposium (ISS), 2015, pp. 1-10: IEEE.

[28] L. Iozan, M. Kirkko-Jaakkola, J. Collin, J. Takala, and C. Rusu, "Using a MEMS gyroscope to measure the Earth's rotation for gyrocompassing applications," Measurement Science and Technology, vol. 23, no. 2, p. 025005, 2012.

[29] E.-H. Shin and N. El-Sheimy, "Accuracy improvement of low cost INS/GPS for land applications," in

Proceedings of the 2002 national technical meeting of the institute of navigation, 2002, pp. 146-157.
[30] D. Titterton, J. L. Weston, and J. Weston, Strapdown inertial navigation technology. IET, 2004.
[31] K. R. Britting, "Inertial navigation systems analysis," 1971.
[32] J. Farrell, Aided navigation: GPS with high rate sensors. McGraw-Hill, Inc., 2008.